BIOCYBERNETICS AND BIOMEDICAL ENGINEERING 42 (2022) 258–272

Available at www.sciencedirect.com

ScienceDirect

journal homepage: www.elsevier.com/locate/bbe

Original Research Article

A combination of statistical parameters for epileptic seizure detection and classification using VMD and NLTWSVM

Shang Zhang [a], *Guangda Liu* [a,*], *Ruolan Xiao* [a], *Wenjie Cui* [a], *Jing Cai* [a], *Xinlei Hu* [a], *Yubing Sun* [a], *Jiqing Qiu* [b], *Yuan Qi* [b]

[a] *College of Instrumentation and Electrical Engineering, Jilin University, Changchun, China*
[b] *The First Hospital of Jilin University, Changchun, China*

ARTICLE INFO

Article history:
Received 29 August 2021
Received in revised form
22 January 2022
Accepted 9 February 2022
Available online 17 February 2022

Keywords:
Epileptic seizure detection
Variational mode decomposition
Non-linear twin support vector machine
Feature extraction
Seizure type classification

ABSTRACT

The epileptic seizure detection and classification is of great significance for clinical diagnosis and treatment. To realize the detection and classification of epileptic seizure, this paper proposes a method based on the combination of signal decomposition and statistical methods. First, the algorithm of variational mode decomposition (VMD) is applied to extract the components of intrinsic mode functions (IMFs) by decomposing the EEG signals. Then the statistical method is utilized to calculate the eight features of maximum, minimum, average, variance, skewness, kurtosis, coefficient of variation and volatility index for each extracted IMF component. Finally, the best combinations of extracted features are fed into the non-linear twin support vector machine (NLTWSVM) to classify the epileptic signals. The EEG database from University of Bonn is used to confirm the effectiveness of the proposed method for epileptic seizure detection. The final experimental results demonstrate that the classification accuracy can reach 98.86%, 98.37%, 99.02%, 99.41% and 99.57% for the database of C-E, D-E, CD-E, ABCD-E and AB-CD-E, respectively. The TUSZ corpus in the TUH EEG corpus is also used to classify epileptic seizure types using the method in this article. The result is expressed by the confusion matrix and the weighted F_1 score is 0.923, which shows this method has potential to help experienced neurophysiologists classify epileptic seizure types in the clinic.

1. Introduction

Epilepsy is a recurring neurological brain disease and can lead to transient brain dysfunction, which is generally generated from a sudden, severe and hypersynchronous discharge by the abnormal brain neurons [1,2]. According to the World Health Organization (WHO), more than 50 million people suffer from epilepsy all over the world, of which about 80%

* Corresponding author at: College of Instrumentation and Electrical Engineering, Jilin University, Changchun 130000, China.
E-mail address: gdliu@jlu.edu.cn (G. Liu).
https://doi.org/10.1016/j.bbe.2022.02.004
0168-8227/

epileptic patients live in low- and middle-income countries [3]. Epilepsy not only has serious impacts on the patients' life, study, work and spirit, but also endangers the safety of the patients [2,4], especially among children [4] and older people [5]. Electroencephalography (EEG) is a technique to record the brain electrical activity [1]. EEG signals are recorded through invasive electrodes positioned on certain specific locations of the cerebral cortex or non-invasive surface electrodes on the scalp. At present, the experienced neurophysiologists analyze EEG signals for detecting and classifying epileptic seizure by visual examination [6–9]. However, the currently adopted visual examination by trained neurophysiologists is a time-consuming and labor-intensive procedure, and there may be diagnostic errors due to human subjective factors during the examination process [7,10]. Therefore, the epileptic seizure detection and classification is of great significance to the field of clinical diagnosis and treatment.

The EEG signal is a typical non-linear and non-stationary weak biological signal [11]. Thus, the feature extraction and feature classification of EEG signals are currently a research on hot issue of scholars worldwide. The analysis methods of EEG signals can be divided into four categories, including time domain, frequency domain, time–frequency domain and non-linear dynamics [12,13]. The analysis approaches in time–frequency domain and non-linear dynamics are the current mainstream methods. Time-frequency methods such as discrete short-time Fourier transform (DSTFT), discrete wavelet transformation (DWT), wavelet packet transform, Stockwell transform (ST), dual-tree complex wavelet transform (DT-CWT), empirical mode decomposition (EMD), local mean decomposition (LMD) and smoothed pseudo Wigner-Ville distribution (SPWVD) are widely utilized in the field of diagnosis and treatment of epilepsy [9,14–24]. The methods of non-linear dynamics such as entropy, correlation dimension, higher-order moments and fractal dimension are commonly employed in the field of epileptic signal analysis [20,25–27]. In recent years, the combination of time–frequency domain and statistical methods for realizing the feature extraction of epileptic signals has been recognized and valued by scholars [14,20,28–35].

T. Zhang et al. used frequency slice wavelet transform to extract different rhythm signals, and the vectors of features were formed by approximate entropy and fluctuation index, then the support vector machine optimized by genetic algorithms was utilized to classify epileptic signals, and the classification accuracy reached 98.3% [36]. J.-L. Song et al. presented an approach of detection of epileptic seizures based on lagged Poincaré plots and extreme learning machine, and the classification accuracy, sensitivity and specificity attained 96.16%, 96.00% and 96.37%, respectively [37]. M. Sharma et al. described an approach for detecting the epileptic seizures by analytic time–frequency flexible wavelet transform (ATFFWT) and least-squares support vector machine (LS-SVM), and the accuracy, sensitivity and specificity reached 98.67%, 100.00% and 96.00% [20]. J. Jia et al. constructed the growth curve and extracted statistical features using complete ensemble empirical mode decomposition with adaptive noise (CEEMDAN), and the method realized 98.00% accuracy, 100.00% sensitivity and 99.00% specificity by the random forest classifier [38]. Y. Li et al. employed a multiscale radial basis function with a modified particle swarm optimization (MRBF-MPSO) and reported 98.73% accuracy, 98.00% sensitivity and 99.10% specificity for the dataset of S-NF [39].

In 1998, N.E. Huang et al. proposed the approach of EMD, which is appropriate to analyze weak biological signals [40]. EMD can decompose the epileptic signals into the intrinsic mode functions (IMFs) by time scale adaptively. However, this method has some problems such as end effect and mode mixing, which are generated because the error of envelope estimation is gradually amplified when multiple recursive decompositions are performed through the envelope of the extreme point [41]. These problems result in the inability to correctly separate the similar frequency components, and the signal will lose part of the detailed information, which affects the signal integrity and detection accuracy. Moreover, the decomposition error of this method is relatively large when the signal is polluted by noise. Due to the drawback of mode mixing in EMD, Z. Wu and N.E. Huang proposed the method of ensemble empirical mode decomposition (EEMD) by mixing the analysis signal with white noise [42]. The method eliminates the phenomenon of mode mixing and improves noise immunity using the uniform distribution of the power spectrum density of white noise to change the characteristics of extreme points in the frequency domain [43]. However, this method increases the amount of calculation and decomposes the signal into multiple components that exceed the true composition of the original signal.

Due to the above approaches' limitations, K. Dragomiretskiy and D. Zosso proposed a new multi-scale and time–frequency signal analysis decomposition method named variational mode decomposition (VMD) in 2014 [44]. The method introduces the variational model to search for the optimal solutions by iteration to make the sum of the estimated bandwidth of each mode minimized. In the frequency domain, each mode and the corresponding center frequencies are constantly updated so that the algorithm can adaptively extract the narrow-band components, and the decomposed components are also defined as intrinsic mode functions (IMFs), where each component is a stationary amplitude modulation and frequency modulation signal with limited bandwidth [32,45]. This algorithm can effectively avoid the drawback of mode mixing generated by gradual amplification of the estimation error in the recursive process and has certain advantages in calculation speed, decomposition accuracy of complex signals and anti-noise interference.

Considering the characteristics of weak biological signals, this paper uses VMD to extract the decomposed components of epileptic EEG signals. Since statistics can objectively describe the overall quantitative characteristics and quantitative relationships of signals, this article applies statistical methods to extract IMF components' eight features of maximum, minimum, average, variance, skewness, kurtosis, coefficient of variation and volatility index. Then the best combinations of extracted features are fed into the non-linear twin support vector machine (NLTWSVM) for training to realize the detection and classification of epileptic seizure. This proposed method realizes the combination of signal decomposition and statistical analysis for epileptic EEG signals, and it is tested on the public datasets and compared with other similar methods.

2. Materials and methods

2.1. *Database-A*

Database-A uses a publicly available online database from Department of Epileptology, University of Bonn, Germany [46]. The EEG database has been widely used in the epileptic seizure detection. The details of this database are shown in Table 1. The database is composed of five groups of EEG datasets, and each dataset includes 100 segments of EEG signals with a sampling frequency of 173.6 Hz and a duration of 23.6 s.

2.2. *Database-B*

Database-B uses the Temple University Hospital EEG Seizure Corpus (TUSZ, v1.5.2), which contains annotations of occurrence time and epileptic seizure types and includes the patient information such as ID, age, gender, seizure event number and seizure duration in the database [47]. Eight types of epileptic seizures annotated from the database are Focal Non-Specific Seizure (FNSZ), Generalized Non-Specific Seizure (GNSZ), Complex Partial Seizure (CPSZ), Tonic Clonic Seizure (TCSZ), Absence Seizure (ABSZ), Simple Partial Seizure (SPSZ), Tonic Seizure (TNSZ) and Myoclonic Seizure (MYSZ). The database statistics description is shown in Table 2. This database contains two sets, called training set and development set. The training set is used to train the algorithm model, and the development set is used to test the performance of the model.

2.3. *Variational mode decomposition*

Assuming that the input signal $x(t)$ contains k number of IMF components $u_k(t)$ [44]. The method consists of the construction and solution of variational model.

2.3.1. *Construction of variational model*

Essentially, the IMF is defined as a bandwidth-limited amplitude modulation and frequency modulation function [48]. The specific methods of construction are below:

1. Perform Hilbert transform on each IMF component $u_k(t)$ to construct an analytic signal for obtaining its unilateral frequency spectrum;

2. Mix the analytic signal of each IMF component with the index $e^{-j\omega_k t}$ to shift spectrums of IMF components to basebands;

3. Calculate the squared L^2-norm of the gradient of the demodulated signal, estimate corresponding bandwidths of IMF components, and construct a constrained variational model:

$$\begin{cases} \min\limits_{\{u_k\},\{\omega_k\}} \left\{ \sum\limits_k \left\| \partial_t \left[\left(\delta(t) + \frac{j}{\pi t} \right) * u_k(t) \right] e^{-j\omega_k t} \right\|_2^2 \right\} \\ \text{s.t.} \qquad \sum\limits_k u_k(t) = x(t) \end{cases} \tag{1}$$

where δ is the Dirac function, $\{u_k\} = \{u_1, u_2, \cdots, u_K\}$ is the set of all IMF components, $\{\omega_k\} = \{\omega_1, \omega_2, \cdots, \omega_K\}$ is the set of center frequencies, K is the number of IMF components. Equally, $\sum_k = \sum_{k=1}^{K}$ is explained as the summation of all IMF components.

2.3.2. *Solution of variational model*

1. In order to resolve the constrained variational problem, the constructed augmented Lagrangian function expression is proposed based on quadratic penalty term and Lagrangian multiplier:

$$\begin{aligned} \mathscr{L}(\{u_k\}, \{\omega_k\}, \lambda) = \alpha \sum_k \left\| \partial_t \left[\left(\delta(t) + \frac{j}{\pi t} \right) * u_k(t) \right] e^{-j\omega_k t} \right\|_2^2 \\ + \left\| x(t) - \sum_k u_k(t) \right\|_2^2 \\ + \left\langle \lambda(t), x(t) - \sum_k u_k(t) \right\rangle \end{aligned} \tag{2}$$

Among them, the quadratic penalty term α is the limitation index of data-fidelity and the Lagrangian multiplier λ can ensure strict enforcement [49].

2. The alternate direction method of multipliers (ADMM) is applied to search for the saddle point of the augmented Lagrangian found by an alternate update of $u_k^{n+1}(t)$, $\omega_k^{n+1}(t)$ and $\lambda^{n+1}(t)$. This saddle point is the optimal solution of the variational model. The iteration formulas are below:

$$u_k^{n+1} \leftarrow \arg\min_{u_k} \mathscr{L}(\{u_{i<k}^{n+1}\}, \{u_{i\geqslant k}^{n}\}, \{\omega_i^n\}, \lambda^n) \tag{3}$$

$$\omega_k^{n+1} \leftarrow \arg\min_{\omega_k} \mathscr{L}(\{u_i^{n+1}\}, \{\omega_{i<k}^{n+1}\}, \{\omega_{i\geqslant k}^{n}\}, \lambda^n) \tag{4}$$

Table 1 – The details of the Bonn database.

Dataset	Testing object	Record type	Status of testing object	Number of samples	Electrode position
A	Healthy volunteers	Surface	Awake, open eyes	100	10–20 electrode system
B	Healthy volunteers	Surface	Awake, close eyes	100	10–20 electrode system
C	Epileptic patients	Intracranial	Interictal	100	Outside epileptogenic zone
D	Epileptic patients	Intracranial	Interictal	100	Inside epileptogenic zone
E	Epileptic patients	Intracranial	Ictal	100	Inside epileptogenic zone

Table 2 – The statistics description of the TUSZ database.

Seizure type	Patient number	Seizure event number	Seizure duration (sec)
FNSZ	150	1836	121,139
GNSZ	81	583	59,717
CPSZ	41	367	36,321
TCSZ	14	48	5548
ABSZ	12	99	852
SPSZ	3	52	2146
TNSZ	3	62	1204
MYSZ	2	3	1312
Total	306	3050	228,239

$$\lambda^{n+1} \leftarrow \lambda^{n} + \tau\left(x(t) - \sum_k u_k^{n+1}\right) \tag{5}$$

The convergence criterion is defined by:

$$\sum_k \| u_k^{n+1} - u_k^{n} \|_2^2 / \| u_k^{n} \|_2^2 < \varepsilon \tag{6}$$

where τ denotes the Lagrangian multiplier update parameter and ε represents the convergence tolerance.

3. Mode u_k update and solution

Rewrite Eq. (3) as the following equivalent expression:

$$u_k^{n+1} = \underset{u_k \in X}{\operatorname{argmin}} \left\{ \alpha \left\| \partial_t \left[\left(\delta(t) + \frac{j}{\pi t} \right) * u_k(t) \right] e^{-j\omega_k t} \right\|_2^2 + \left\| x(t) - \sum_i u_i(t) + \frac{\lambda(t)}{2} \right\|_2^2 \right\} \tag{7}$$

where ω_k is equal to ω_k^{n+1}, $\sum_i u_i(t)$ is equal to $\sum_{i \neq k} u_i(t)^{n+1}$.

Due to the Parseval/Plancherel Fourier isometry, Eq. (7) is converted into the spectral domain as below:

$$\hat{u}_k^{n+1} = \underset{\hat{u}_k, u_k \in X}{\operatorname{argmin}} \left\{ \alpha \left\| j\omega[(1 + sgn(\omega + \omega_k))\hat{u}_k(\omega + \omega_k)] \right\|_2^2 \right. \\ \left. left + \left\| \hat{x}(\omega) - \sum_i \hat{u}_i(\omega) + \frac{\hat{\lambda}(\omega)}{2} \right\|_2^2 \right\} \tag{8}$$

Replace ω in Eq. (8) of penalty term with $\omega - \omega_k$, the expression is replaced as follows:

$$\hat{u}_k^{n+1} = \underset{\hat{u}_k, u_k \in X}{\operatorname{argmin}} \left\{ \alpha \left\| j(\omega - \omega_k)[(1 + sgn(\omega))\hat{u}_k(\omega)] \right\|_2^2 \right. \\ \left. + \left\| \hat{x}(\omega) - \sum_i \hat{u}_i(\omega) + \frac{\hat{\lambda}(\omega)}{2} \right\|_2^2 \right\} \tag{9}$$

Since the real signals have the characteristic of Hermitian symmetry, Eq. (9) can be changed to half-space integrals over the non-negative frequencies as below:

$$\hat{u}_k^{n+1} = \underset{\hat{u}_k, u_k \in X}{\operatorname{argmin}} \left\{ \int_0^{\infty} 4\alpha(\omega - \omega_k)^2 |\hat{u}_k(\omega)|^2 + 2\left| \hat{x}(\omega) - \sum_i \hat{u}_i(\omega) + \frac{\hat{\lambda}(\omega)}{2} \right|^2 d\omega \right\} \tag{10}$$

Solving Eq. (10) as a quadratic optimization problem, the above expression can be further described as:

$$\hat{u}_k^{n+1}(\omega) = \frac{\hat{x}(\omega) - \sum_{i \neq k} \hat{u}_i(\omega) + \frac{\hat{\lambda}(\omega)}{2}}{1 + 2\alpha(\omega - \omega_k)^2} \tag{11}$$

4. Center frequency ω_k update and solution

Rewrite Eq. (4) as the following equivalent expression:

$$\omega_k^{n+1} = \underset{\omega_k}{\operatorname{argmin}} \left\{ \left\| \partial_t \left[\left(\delta(t) + \frac{j}{\pi t} \right) * u_k(t) \right] e^{-j\omega_k t} \right\|_2^2 \right\} \tag{12}$$

According to the same process, Eq. (12) is transformed as below:

$$\omega_k^{n+1} = \underset{\omega_k}{\operatorname{argmin}} \left\{ \int_0^{\infty} (\omega - \omega_k)^2 |\hat{u}_k(\omega)|^2 d\omega \right\} \tag{13}$$

Solving Eq. (13) as a quadratic optimization problem, the above expression can be further represented as:

$$\omega_k^{n+1} = \frac{\int_0^{\infty} \omega |\hat{u}_k(\omega)|^2 d\omega}{\int_0^{\infty} |\hat{u}_k(\omega)|^2 d\omega} \tag{14}$$

2.4. *EEG feature extraction*

In the paper, the original EEG signals are decomposed by the VMD algorithm to obtain the IMF components, and feature extraction is performed to acquire eight features of maximum, minimum, average, variance, skewness, kurtosis, coefficient of variation and volatility index.

Assuming that the signal $u_k(t)$ obtained by decomposing the EEG signal $x(t)$ through VMD is a time series of length L, the extracted features are shown in Table 3.

2.5. *Twin support vector machine*

In recent years, Twin support vector machine (TWSVM), as an extension of support vector machine (SVM), has received extensive attention. The difference from the traditional SVM algorithm is that TWSVM constructs a corresponding supporting hyperplane for each category, and each hyperplane is as close as possible to the data points of the corresponding class and far away from the data points of other classes [50]. TWSVM is not limited to whether the hyperplane is parallel and the size of the interval. Compared with SVM, TWSVM has more advantages in the effect of classification and speed calculation.

For the classifier of linear twin support vector machine (LTWSVM), consider the problem of binary classification with training samples, including p positive samples and q negative samples, the expression is as follows:

$$T = \{(x_1, +1), (x_2, +1), \cdots (x_p, +1), (x_{p+1}, -1), (x_{p+2}, -1), \cdots (x_{p+q}, -1)\} \tag{15}$$

where $x_i \in R^n, i = 1, 2, \cdots, p + q$. LTWSVM seeks a pair of non-parallel hyperplanes as follows:

$$\begin{aligned} (\omega_+ \cdot x) + b_+ = 0 \\ (\omega_- \cdot x) + b_- = 0 \end{aligned} \tag{16}$$

where $\omega_+, \omega_- \in R^n$, $b_+, b_- \in R$. In order to acquire the pair of hyperplanes, two primal quadratic programming problems (QPPs) are described below:

Table 3 – Extracted features used in this work.

Feature name	Mathematical formulation
Maximum (Max)	$Max = \max(u_k(t))$
Minimum (Min)	$Min = \min(u_k(t))$
Average (Ave)	$Ave = \frac{1}{L}\sum_{i=1}^{L} u_{k,i}(t)$
Variance (Var)	$Var = \frac{1}{L-1}\sum_{i=1}^{L}(u_{k,i}(t) - Ave)^2$
Skewness (Skew)	$Skew = \frac{1}{L}\sum_{i=1}^{L}\left(\frac{u_{k,i}(t)-Ave}{Var^{1/2}}\right)^3$
Kurtosis (Kurt)	$Kurt = \frac{1}{L-1}\sum_{i=1}^{L}(u_{k,i}(t) - Ave)^4/Var^2 - 3$
Coefficient of variation (CV)	$CV = \frac{Var}{Ave^2}$
Volatility index (VI)	$VI = \frac{1}{L}\sum_{i=1}^{L-1}\lvert u_{k,i+1}(t) - u_{k,i}(t)\rvert$

$$\begin{aligned} &\min_{\omega_+,b_+,\xi_-} \tfrac{1}{2}(A\omega_+ + e_+b_+)^T(A\omega_+ + e_+b_+) + c_1e_-^T\xi_- \\ &\quad \text{s.t.} \ -(B\omega_+ + e_-b_+) + \xi_- \geqslant e_-, \xi_- \geqslant 0 \end{aligned} \tag{17}$$

And

$$\begin{aligned} &\min_{\omega_-,b_-,\xi_+} \tfrac{1}{2}(B\omega_- + e_-b_-)^T(B\omega_- + e_-b_-) + c_2e_+^T\xi_+ \\ &\quad \text{s.t.} \ (A\omega_- + e_+b_-) + \xi_+ \geqslant e_+, \xi_+ \geqslant 0 \end{aligned} \tag{18}$$

where $A = (x_1, x_2, \cdots, x_p)^T \in R^{p\times n}$, $B = (x_{p+1}, x_{p+2}, \cdots, x_{p+q})^T \in R^{q\times n}$, and $l = p + q$. e_+ and e_- are the column vectors of ones of appropriate dimensions. ξ_+ and ξ_- are slack vectors. c_1 and c_2 are penalty parameters, which are used to penalize a few linearly inseparable samples to maximize the separability of samples. The dual problems are as follows:

$$\begin{aligned} &\max_{\alpha} \ e_-^T\alpha - \tfrac{1}{2}\alpha^T G(H^TH)^{-1}G^T\alpha \\ &\quad \text{s.t.} \ 0 \leqslant \alpha \leqslant c_1e_- \end{aligned} \tag{19}$$

And

$$\begin{aligned} &\max_{\gamma} \ e_+^T\gamma - \tfrac{1}{2}\gamma^T H(G^TG)^{-1}H^T\gamma \\ &\quad \text{s.t.} \ 0 \leqslant \gamma \leqslant c_2e_+ \end{aligned} \tag{20}$$

where $H = [A \quad e_+] \in R^{p\times(n+1)}$, $G = [B \quad e_-] \in R^{q\times(n+1)}$.

The non-parallel hyperplanes can be acquired by the solutions to the QPPs of Eq. (17) and Eq. (18), as the following formulations:

$$\begin{aligned} (\omega_+^T, b_+)^T &= -(H^TH)^{-1}G^T\alpha \\ (\omega_-^T, b_-)^T &= -(G^TG)^{-1}H^T\gamma \end{aligned} \tag{21}$$

For a new input $x \in R^n$, its discrimination function of the category is described as:

$$Class = \arg\min_{k=-,+} \lvert(\omega_k \cdot x) + b_k\rvert \tag{22}$$

where $\lvert\cdot\rvert$ denotes the perpendicular distance of the sample x from the hyperplane.

For the classifier of non-linear twin support vector machine (NLTWSVM), the kernel functions are applied to convert linear inseparable problems of original space to linear separable problems of high-dimensional space [51]. NLTWSVM still searches for a pair of non-parallel hyperplanes below:

$$\begin{aligned} K(x^T, C^T)u_+ + b_+ = 0 \\ K(x^T, C^T)u_- + b_- = 0 \end{aligned} \tag{23}$$

where $C^T = [A; B]^T \in R^{n\times l}$, $K(\cdot,\cdot)$ stands for an appropriate kernel function, and the QPPs can be described below:

$$\begin{aligned} &\min_{u_+,b_+,\xi_-} \tfrac{1}{2}\| K(A, C^T)u_+ + e_+b_+ \|^2 + c_1e_-^T\xi_- \\ &\text{s.t.} \ -(K(B, C^T)u_+ + e_-b_+) + \xi_- \geqslant e_-, \xi_- \geqslant 0 \end{aligned} \tag{24}$$

And

$$\begin{aligned} &\min_{u_-,b_-,\xi_+} \tfrac{1}{2}\| K(B, C^T)u_- + e_-b_- \|^2 + c_2e_+^T\xi_+ \\ &\text{s.t.} \ (K(A, C^T)u_- + e_+b_-) + \xi_+ \geqslant e_+, \xi_+ \geqslant 0 \end{aligned} \tag{25}$$

The dual formulations of the corresponding dual problems are below:

$$\begin{aligned} &\max_{\alpha} \ e_-^T\alpha - \tfrac{1}{2}\alpha^T R(S^TS)^{-1}R^T\alpha \\ &\quad \text{s.t.} \ 0 \leqslant \alpha \leqslant c_1e_- \end{aligned} \tag{26}$$

And

$$\begin{aligned} &\max_{\gamma} \ e_+^T\gamma - \tfrac{1}{2}\gamma^T S(R^TR)^{-1}S^T\gamma \\ &\quad \text{s.t.} \ 0 \leqslant \gamma \leqslant c_2e_+ \end{aligned} \tag{27}$$

where $S = [K(A, C^T)e_+]$, $R = [K(B, C^T)e_-]$.

The non-parallel hyperplanes can be acquired by the solutions to the QPPs of Eq. (24) and Eq. (25), as the following formulations:

$$\begin{aligned} (u_+^T, b_+)^T &= -(S^TS)^{-1}R^T\alpha \\ (u_-^T, b_-)^T &= -(R^TR)^{-1}S^T\gamma \end{aligned} \tag{28}$$

For a new input $x \in R^n$, its discrimination function of the category is described as:

$$Class = \arg\min_{k=-,+} \lvert K(x^T, C^T)u_k + b_k\rvert \tag{29}$$

3. Experiments and results

3.1. Experimental design

For database-A, the experiment selects all segments of EEG signals from the selected datasets and divides the first 23 s EEG data of each segment into 23 data fragment samples with one second as a unit. And each extracted data fragment sample is decomposed by VMD algorithm to acquire the corresponding IMF components, then the eight features of each

IMF component are extracted to obtain the maximum, minimum, average, variance, skewness, kurtosis, coefficient of variation and volatility index. The datasets generate five combination cases to test the classification effect and analyze the combinations' impact of different datasets, and the combination cases are shown in Table 4.

For database-B, since the seizure event number of seizure type of MYSZ is too small, we eliminate this seizure type and use the remaining seven seizure types to build a model for the 7-class classification. Perform a 60 Hz notch and a band-pass filter from 0.1 Hz to 80 Hz on the EEG data of the remaining 7 seizure types within the seizure event time, and then extract the FP1-FP2 electrode channel EEG data from the processed data. The EEG data fragments are extracted by dividing the processed data with a time interval of 1 s. The data fragments extracted in the training set are used as the model training set, and the data fragments extracted in the development set are used for model testing. The algorithm performs 4-layer VMD decomposition to acquire IMF components and extracts eight types of features from IMF components, and then inputs features to the NLTWSVM for multi-class training and testing.

The proposed approach for the epileptic seizure detection and classification is described in Fig. 1. All the experiments implement on the same PC with Intel-core i3-9100F CPU@3.60 GHz processor-based machine with 8 GB RAM using Python 3.6. The representative original EEG signals in the datasets corresponding to the three statuses of normal, interictal and ictal periods are presented in Fig. 2.

The IMF components k and quadratic penalty term α are important parameters that affect the results of classification. If the number of k in the algorithm is less than theoretical components, the signals will not be completely decomposed, resulting in under-decomposition; if the number of k is greater than theoretical components, unreasonable false components will be produced, leading to over-decomposition. When k is constant and α is small, the spectra of two adjacent mode functions will be partially overlapped; as α increases, the passband becomes narrower and narrower, which will result in a larger error for reconstructing signals [52]. Therefore, it is important to acquire a reasonable number of IMF components k and quadratic penalty term α for signal decomposition. In this paper, the different numbers of k and α are analyzed, and the experiments determine that the number of k is 4 and α is 2000.

In the paper, the classifier of NLTWSVM is selected to classify the samples, and the radial basis function is selected as kernel function as follows:

$$K(x, x_i) = \exp\left(\frac{-\| x - x_i \|^2}{2\sigma^2}\right) \tag{30}$$

Table 4 – Combination cases from the database-A.

Combination case	Classes type
C vs. E	Interictal vs. ictal
D vs. E	Interictal vs. ictal
CD vs. E	Interictal vs. ictal
ABCD vs. E	Non-ictal vs. ictal
AB vs. CD vs. E	Healthy vs. interictal vs. ictal

where σ represents the width of function. In this paper, different parameters are tested to observe the classification effect, and the parameters which obtain the best classification accuracy are chosen as the used classifiers' parameters for each combination case.

3.2. *Results*

In this paper, four-layer VMD decomposition is applied to data fragment samples to acquire IMF components. The representative EEG data fragment samples and the corresponding IMF components of three statuses of normal, interictal and ictal periods are shown in Fig. 3. It illustrates that the IMF components of each order obtained from the VMD decomposition represent different characteristic compositions in the original EEG signal, and the EEG amplitude of the ictal period is higher than that of normal and interictal periods.

After VMD decomposition is applied to acquire IMF components of the EEG data fragment samples, the corresponding eight features of maximum, minimum, average, variance, skewness, kurtosis, coefficient of variation and volatility index are calculated for each IMF component. Fig. 4 shows the eight features' box plots of IMF1, IMF2, IMF3 and IMF4 obtained from VMD decomposition in five datasets of normal, interictal and ictal periods. Among them, the black, red, blue and green colors represent the corresponding features' box plots of IMF1, IMF2, IMF3 and IMF4, respectively. It can be seen the IMF components of each order during the ictal period have significant differences compared with the IMF components of the normal and interictal periods for each extracted feature. These differences establish a good foundation for detecting epileptic seizure accurately.

The performance of the classifier is evaluated by the evaluation parameters named sensitivity (SEN), specificity (SPEC) and accuracy (ACC) [53,54]. To ensure the effectiveness of the classification results, the 10-fold cross-validation method is applied to the experiments described in this article. The evaluation parameters are calculated below:

$$\begin{aligned} SEN &= \tfrac{TP}{TP+FN} \\ SPEC &= \tfrac{TN}{TN+FP} \\ ACC &= \tfrac{TP+TN}{TP+FP+TN+FN} \end{aligned} \tag{31}$$

For the 7-class classification problem proposed in this paper, the weighted F_1 score is used to evaluate the performance of the classifier. The formula is as follows:

$$\begin{aligned} Precision &= \tfrac{TP}{TP+FP} \\ Weighted\ F_1 &= \sum_{i=1}^{7} \tfrac{2*Precision_i*Sensitivity_i}{Precision_i+Sensitivity_i} * \omega_i \end{aligned} \tag{32}$$

where ω_i is the weight of positive samples in the i-th class.

In order to test the impact and classification effect for the selected features, the different feature numbers and types of the eight extracted features are selected to train each combination case in turn, and the best feature combinations and the corresponding evaluation parameters of each combination case are shown in Table 5.

It can be seen from Table 5 that the classification accuracy can reach 98.86%, 98.37%, 99.02%, 99.41% and 99.57% for the database of C-E, D-E, CD-E, ABCD-E and AB-CD-E under the

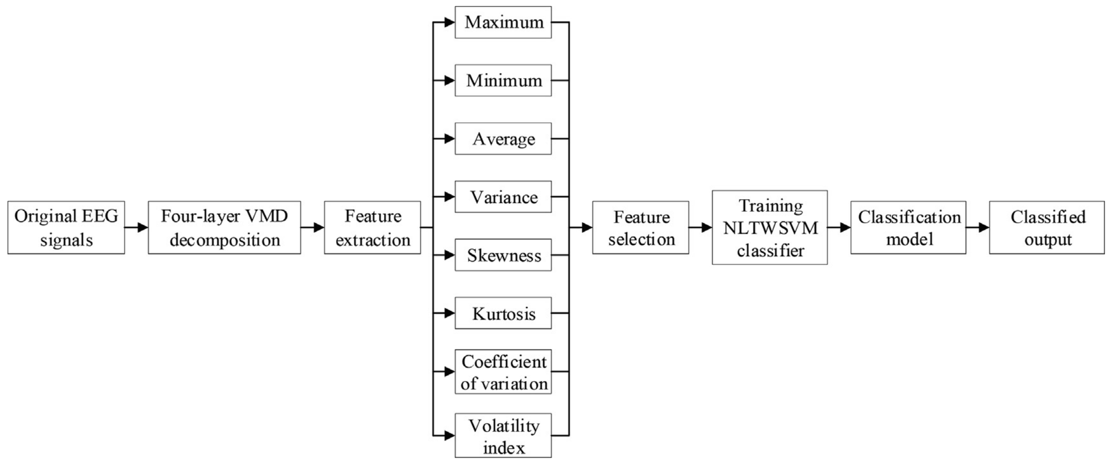

Fig. 1 – Block diagram of the proposed method for the epileptic seizure detection and classification.

best feature combination, respectively. The best feature combinations of each combination case are fed into the used classifiers for training, which can better describe the characteristics of epileptic signals and improve the classification effect.

For multi-classification problems, this article uses the confusion matrix representation method to illustrate the classification effect. The result of the confusion matrix of 7-class classification is shown in Fig. 5. It illustrates that the correct classification of seizure types FNSZ, GNSZ, SPSZ, CPSZ, ABSZ, TNSZ and TCSZ reaches 0.93, 0.93, 0.89, 0.90, 0.97, 0.98 and 0.86 respectively. For the 7-class classification problem, the weighted F_1 score is 0.923. Judging from the classification results, this method can assist experienced neurophysiologists to help identify the seizure type clinically.

4. Discussion

In the article, the classification methods of SVM, LTWSVM and NLTWSVM are applied to compare classification effects. Table 6 illustrates the best evaluation parameters obtained from the different feature numbers and types using the classifiers of SVM, LTWSVM and NLTWSVM for each combination case. It can be seen the proposed classifier of NLTWSVM has the best classification accuracy, sensitivity and specificity than those of other classifiers. The significant improvements in classification accuracy, sensitivity and specificity indicate that the proposed method is conducive to the realization of epileptic seizure detection.

Tables 7–11 present the classification results of the proposed method and the existing methods for the database of C-E, D-E, CD-E, ABCD-E and AB-CD-E. The above tables indicate that the overall classification results of the five combination cases have better results than other algorithms. Therefore, the proposed method is suitable for epileptic seizure detection.

D. Ahmedt-Aristizabal proposed the method based on neural memory networks (NMNs) and external memory model to classify the TUSZ corpus for 7-class classification, and the result of seizure types classification was described by the confusion matrix [67]. The probability of correct classification of the 7 types differed greatly from the confusion matrix, with the lowest being 0.33 and the highest being 1.00. The seizure durations of the SPSZ, TNSZ and TCSZ types in the TUSZ corpus are less than other types, which is challenging for the classifier to classify correctly. The NMNs model had a low correct classification on the above three types, up to 0.50. The number of correct classifications of the above three types of data by the classification method proposed in our article has been reduced, but the minimum correct classification is 0.86, which proves that the method in this paper has a good classification effect on such data types with small seizure durations and has the potential for clinical use.

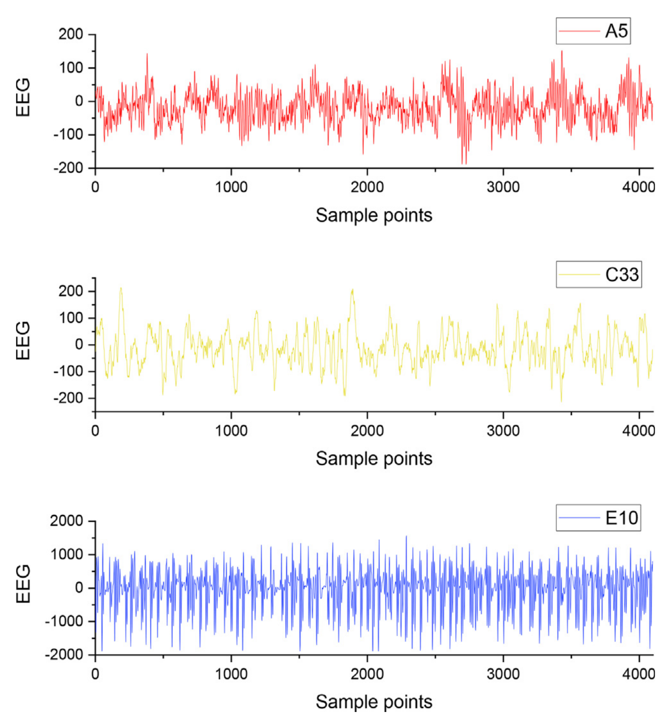

Fig. 2 – The representative original data of normal (A5), interictal (C33) and ictal (E10) EEG signals.

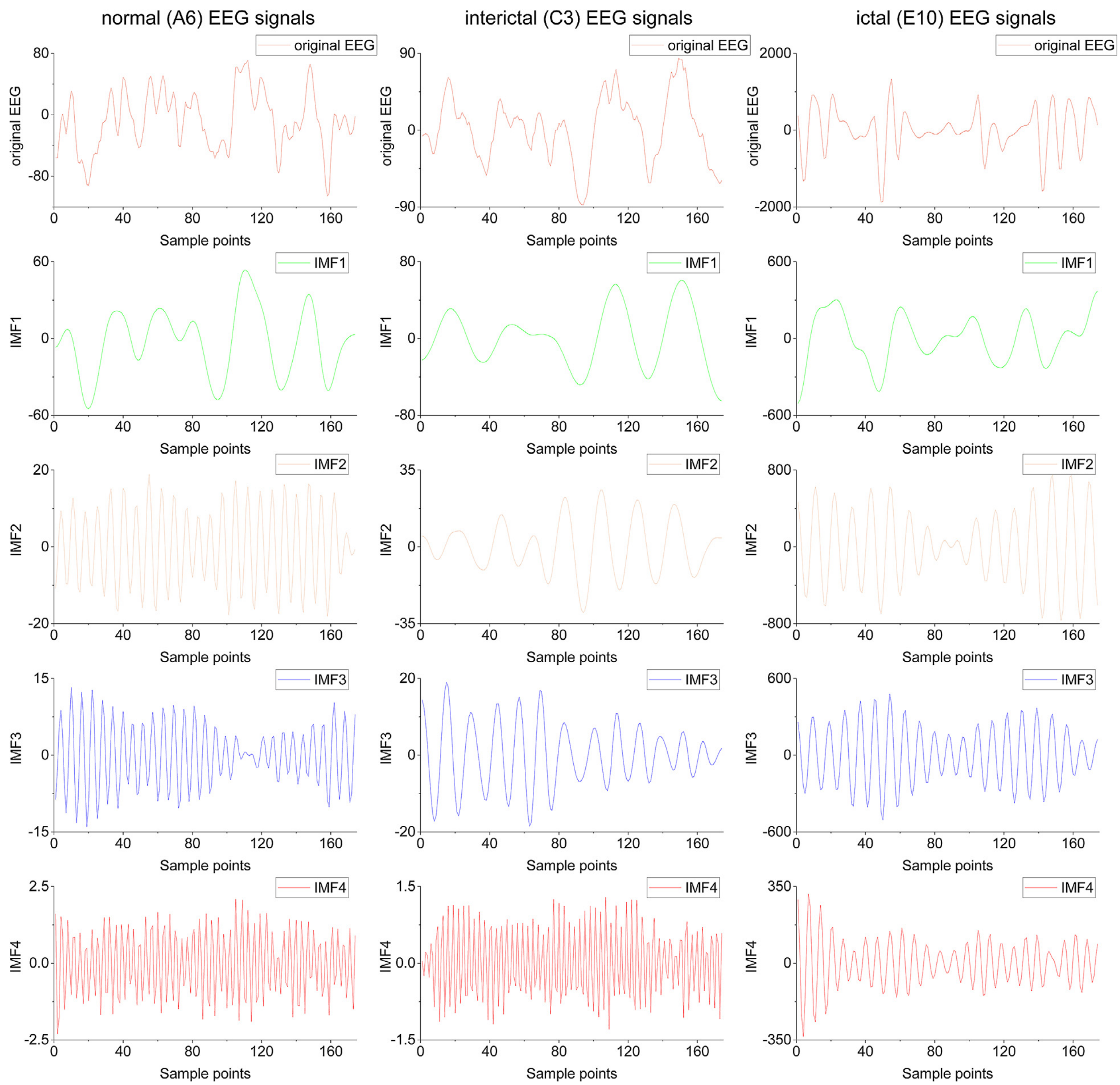

Fig. 3 – The representative EEG data fragment samples and the corresponding IMF components of normal (A6), interictal (C3) and ictal (E10) EEG signals.

N. McCallan used a bagged tree classifier to classify the TUSZ corpus [68]. The first classification objects are FNSZ, GNSZ and NNSZ. From the confusion matrix, the correct classifications of FNSZ, GNSZ and NNSZ can be obtained up to 0.85, 0.74 and 0.64, respectively. The correct classification of FNSZ and GNSZ can both reach 0.93 by the method proposed in our article, which has a better classification effect for these types. The second classification objects are ABSZ, CPSZ, MYSZ, NNSZ, SPSZ, TCSZ and TNSZ. The correct classifications are 0.80, 0.84, 0.34, 0.66, 0.10, 0.47 and 0.53 for the above types, which shows the classification results of ABSZ, CPSZ and NNSZ are better. Compared with the results, our article has higher correct classification results for each type, which can form an effective identification of epileptic seizure types and is helpful for clinical application.

U. Asif used the TUSZ corpus to automatically classify the seizure types [69]. The deep learning framework SeizureNet with multi-spectral feature learning method was utilized to classify 7-class classification problems, and the correct classification of seizure types FNSZ, CPSZ, GNSZ, ABSZ, SPSZ, TNSZ and TCSZ reached 0.93, 0.94, 0.93, 1.00, 0.88, 1.00 and 0.70 respectively. It can be seen from the confusion matrix that the correct classification of TCSZ type is low. Compared with our article, the correct classification of TCSZ type can reach 0.86, which describes that our method can stably classify each type.

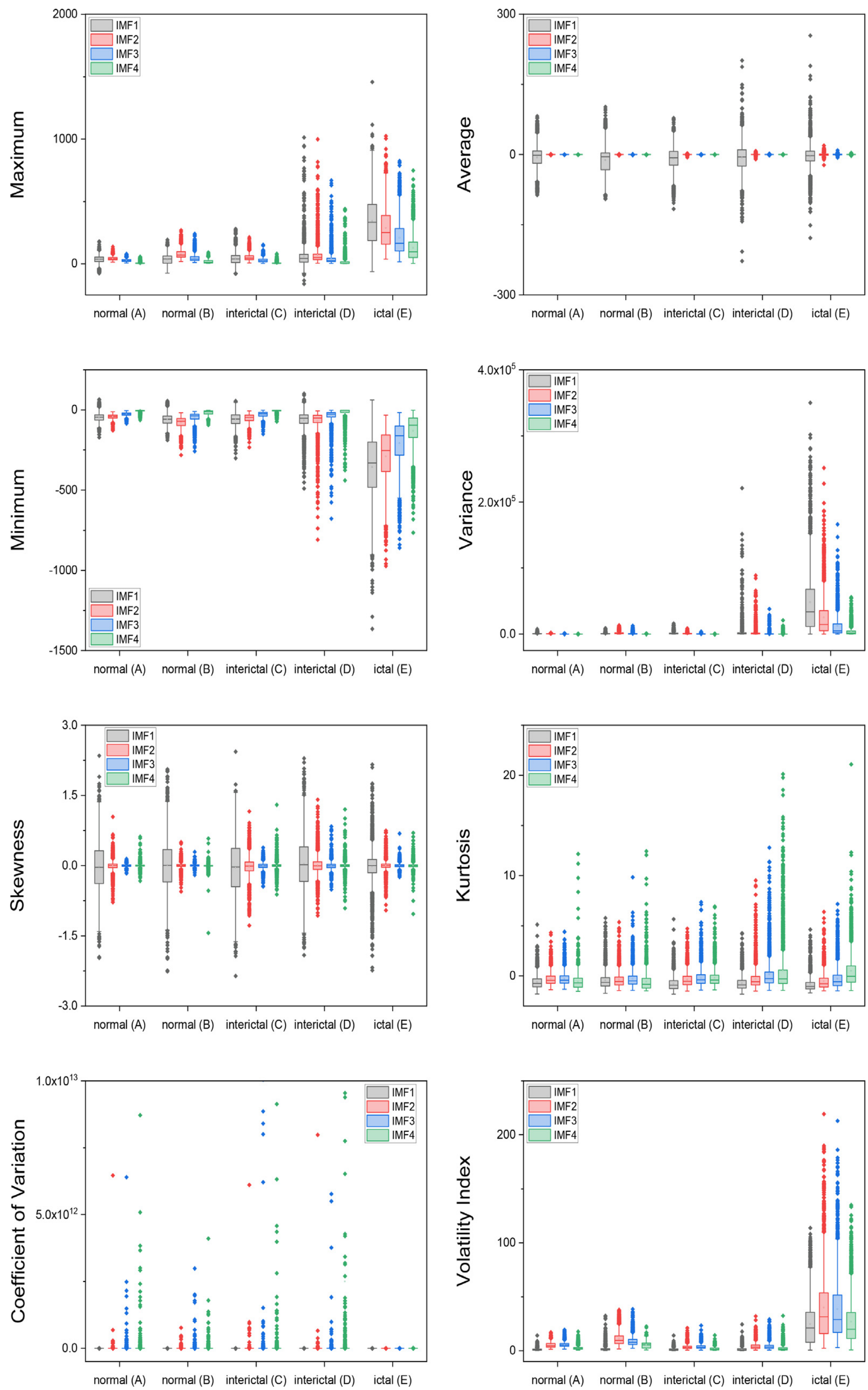

Fig. 4 – The features' box plots of IMF1, IMF2, IMF3 and IMF4 in five datasets of normal, interictal and ictal periods.

Table 5 – The best feature combinations and evaluation parameters results for each combination case.

Combination case	Best feature combination	SEN (%)	SPEC (%)	ACC (%)
C vs. E	Max + Min + Ave + CV + VI	99.02	98.70	98.86
D vs. E	Ave + Var + Skew + Kurt + CV + VI	98.64	98.10	98.37
CD vs. E	Max + Ave + Skew + Kurt + CV + VI	99.13	98.97	99.02
ABCD vs. E	Min + Ave + Var + Skew + CV + VI	99.24	99.46	99.41
AB vs. CD vs. E	Max + Min + Skew + Kurt + CV + VI	99.28	99.66	99.57

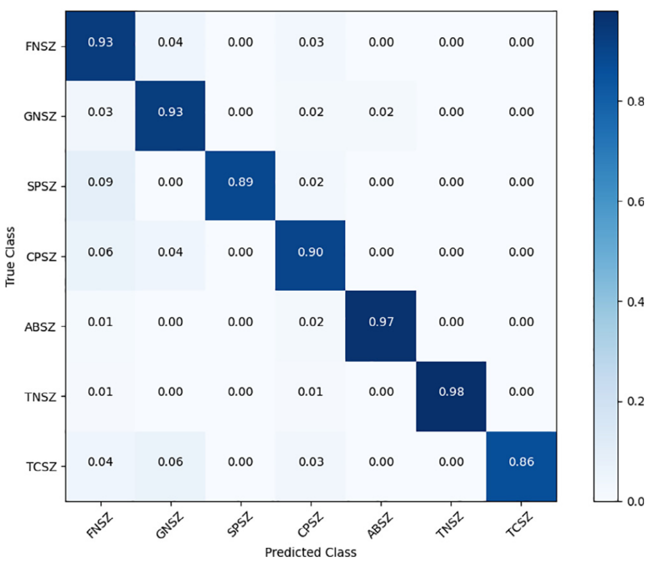

Fig. 5 – The result of the confusion matrix of 7-class classification.

There are many epileptic researches directions that can be used as future research priorities. The detection of epileptic spikes is one direction. K. Fukumori proposed a model called recurrent neural network with self-attention that can detect epileptic spikes without using spike candidates. The average accuracy and F1 value of the classifier reached 90.2% and 88.7% [70]. Detecting and classifying epileptiform discharges is another research direction. C. Lourenco used deep learning method of VGG to detect interictal epileptiform discharges and reported 79% sensitivity and 99% specificity [71]. J.H. Seo used the dynamic mode decomposition to catch the frequency phase transition and realized the identification of ictal and interictal patterns [24]. M.O. Baud found that epileptiform activities display fluctuating dynamics with patient-specific circadian and multidien periodicities, which make signal acquisition and analysis difficult [72].

Epileptic seizure prediction is part of future work. Predicting epileptic seizures can warn epilepsy patients and experienced neurophysiologists of seizure risk, which can help physicians refer to prescribing drugs to epileptic patients to control epileptic seizures and remind epileptic patients to pay attention to their own safety. T. Proix analyzed the recorded RNS intracerebral EEG signals and realized the prediction of epileptic seizures days in advance by the method based on multiday cycles [73]. F. Turco indicated that the maximum length and the mean duration of generalized epileptiform discharges from prolonged ambulatory EEG can predict seizure recurrences [74].

5. Conclusion

In this paper, a new method based on VMD and NLTWSVM is proposed for epileptic seizure detection and classification. This study introduces variational mode decomposition into the analysis of epileptic EEG signals and calculates the IMF components obtained from VMD to extract eight features of maximum, minimum, average, variance, skewness, kurtosis, coefficient of variation and volatility index, then the best

Table 6 – The best evaluation parameters (%) results of various classifiers for each combination case.

Classifier	Index	Combination case				
		C vs. E	D vs. E	CD vs. E	ABCD vs. E	AB vs. CD vs. E
SVM	SEN	94.56	92.39	91.30	92.50	90.58
	SPEC	96.41	94.02	95.49	92.91	94.99
	ACC	95.49	93.21	94.09	92.83	93.33
LTWSVM	SEN	97.32	97.09	98.01	98.29	95.60
	SPEC	96.79	96.52	97.77	97.95	97.54
	ACC	97.05	96.80	97.85	98.02	96.88
NLTWSVM	SEN	99.02	98.64	99.13	99.24	99.28
	SPEC	98.70	98.10	98.97	99.46	99.66
	ACC	98.86	98.37	99.02	99.41	99.57

Table 7 – The classification results of different methods for database C vs. E.

Authors	Methods	SEN (%)	SPEC (%)	ACC (%)
M. Sameer et al. [34]	Short-time Fourier transform + Adaboost	–	–	98.00
S. Siuly et al. [35]	Hermite Transform + LS-SVM	98.18	99.09	98.50
S. Raghu et al. [55]	Multi-features + MLP	–	–	97.68
A. Gupta et al. [56]	Discrete cosine transform + SVM	98.00	97.00	97.50
P. Swami et al. [9]	DT-CWT + General regression neural network	97.55	99.00	98.28
S. Raghu et al. [57]	Matrix determinant + MLP	95.75	99.45	97.60
P. Mathur et al. [58]	Ramanujan periodic subspace + SVM	97.00	99.00	98.00
Proposed method	VMD + NLTWSVM	99.02	98.70	98.86

Table 8 – The classification results of different methods for database D vs. E.

Authors	Methods	SEN (%)	SPEC (%)	ACC (%)
J.-L. Song et al. [37]	Lagged Poincaré plots + ELM	96.00	96.37	96.16
M. Sameer et al. [34]	Short-time Fourier transform + Adaboost	–	–	95.50
S. Siuly et al. [35]	Hermite Transform + LS-SVM	98.09	97.18	97.50
S. Raghu et al. [55]	Multi-features + MLP	–	–	94.56
Y. Li et al. [39]	MRBF-MPSO + SVM	96.80	97.20	97.60
T. Zhang et al. [19]	LMD + SVM optimized by genetic algorithm	98.80	97.40	98.10
A. Gupta et al. [56]	Discrete cosine transform + SVM	96.50	96.20	96.35
S. Raghu et al. [57]	Matrix determinant + MLP	95.80	99.40	97.60
A.R. Hassan et al. [59]	CEEMDAN + Linear programming boosting	97.40	98.25	97.00
P. Mathur et al. [58]	Ramanujan periodic subspace + SVM	95.00	100.00	97.50
Proposed method	VMD + NLTWSVM	98.64	98.10	98.37

combination of extracted features is fed into the non-linear twin support vector machine for training and testing to complete epileptic seizure detection and classification. Since the clinical diagnosis and treatment for epileptic patients are mainly carried out by trained neurophysiologists using EEG through visual examination, the visual examination is still a time-consuming, labor-intensive and inefficient procedure. The proposed method for epileptic seizure detection and classification can clinically reduce neurophysiologists' workload and improve work efficiency. In the experimental results, the classification accuracy can reach 98.86%, 98.37%, 99.02%, 99.41% and 99.57% for the database of C-E, D-E, CD-E, ABCD-E and AB-CD-E. The three indicators of accuracy, sensitivity and specificity of our proposed method have achieved good performance results compared to other existing methods, which proves that the method in this article is effective in detecting epileptic seizures. Moreover, compared with the classifiers of LTWSVM and SVM, the three indicators of the NLTWSVM classifier used in this article have significantly improved in all the combination cases, which further proves

Table 9 – The classification results of different methods for database CD vs. E.

Authors	Methods	SEN (%)	SPEC (%)	ACC (%)
M. Sameer et al. [34]	Short-time Fourier transform + Adaboost	–	–	96.33
S. Raghu et al. [55]	Multi-features + MLP	–	–	84.58
M. Sharma et al. [60]	Orthogonal wavelet filter banks + SVM	98.00	99.00	99.00
Y. Li et al. [39]	MRBF-MPSO + SVM	98.00	99.10	98.73
S. Siuly et al. [35]	Hermite Transform + LS-SVM	97.18	98.54	98.00
P. Swami et al. [9]	DT-CWT + General regression neural network	91.74	96.64	95.00
A. Gupta et al. [56]	Discrete cosine transform + SVM	96.85	97.00	96.92
A.K. Jaiswal et al. [61]	One-dimensional Local Gradient Pattern + ANN	97.20	99.57	98.78
S. Raghu et al. [57]	Matrix determinant + MLP	97.60	94.30	96.95
M. Mursalin et al. [14]	DWT + RF	98.70	98.70	98.67
S. Patidar et al. [62]	Tunable-Q wavelet transform + LS-SVM	97.00	99.00	97.75
M. Sharma et al. [20]	ATFFWT + LS-SVM	100.00	96.00	98.67
B. Mandhouj et al. [63]	STFT + CNN	100.00	98.33	98.88
S.M. Beeraka et al. [29]	STFT + CNN	98.99	93.51	98.17
Proposed method	VMD + NLTWSVM	99.13	98.97	99.02

Table 10 – The classification results of different methods for database ABCD vs. E.

Authors	Methods	SEN (%)	SPEC (%)	ACC (%)
M. Sameer et al. [34]	Short-time Fourier transform + Adaboost	–	–	97.40
W. Zhao et al. [64]	Convolutional neural network	97.00	100.00	99.40
M. Sharma et al. [60]	Orthogonal wavelet filter banks + SVM	98.00	99.75	99.20
P. Swami et al. [9]	DT-CWT + General regression neural network	–	–	96.87
S. Siuly et al. [35]	Hermite Transform + LS-SVM	96.31	98.06	97.60
V. Bajaj et al. [23]	SPWVD + LS-SVM	97.87	98.03	98.00
M.Y. Li et al. [33]	Maximal overlap DWT + RF	98.20	99.33	99.10
A.S.M. Murugavel et al. [65]	Wavelet transform + Hierarchical multi-class SVM	–	–	99.00
T. Zhang et al. [19]	LMD + SVM optimized by genetic algorithm	99.25	97.33	98.87
A. Gupta et al. [56]	Discrete cosine transform + SVM	97.97	97.60	97.79
A.K. Jaiswal et al. [61]	Local neighbor descriptive pattern + ANN	98.30	98.82	98.72
S. Raghu et al. [57]	Matrix determinant + MLP	97.90	96.50	97.20
A.R. Hassan et al. [59]	CEEMDAN + Linear programming boosting	99.17	99.04	99.20
M. Mursalin et al. [14]	DWT + RF	97.40	97.50	97.40
M. Sharma et al. [20]	ATFFWT + LS-SVM	100.00	96.00	99.20
A.R. Hassan et al. [43]	CEEMDAN + Adaptive Boosting	98.75	98.75	99.20
Sukriti et al. [52]	VMD + RF	99.10	100.00	99.30
Y. Kumar et al. [18]	DWT + SVM	98.10	94.40	97.38
K. Samiee et al. [17]	DSTFT + MLP	99.20	93.80	98.10
B. Mandhouj et al. [63]	STFT + CNN	93.33	100.00	98.66
Proposed method	VMD + NLTWSVM	99.24	99.46	99.41

Table 11 – The classification results of different methods for database AB vs. CD vs. E.

Authors	Methods	SEN (%)	SPEC (%)	ACC (%)
Sukriti et al. [52]	VMD + RF	98.20	99.70	98.70
W. Zhao et al. [64]	Convolutional neural network	95.40	97.70	97.07
B. Mandhouj et al. [63]	STFT + CNN	97.78	98.61	98.22
Y. Jiang et al. [66]	Synchroextracting chirplet transform + SVM	–	–	99.33
S. Raghu et al. [57]	Matrix determinant + MLP	96.88	95.50	96.19
A.R. Hassan et al. [43]	CEEMDAN + Adaptive Boosting	97.67	97.35	97.60
T. Zhang et al. [19]	LMD + SVM optimized by genetic algorithm	98.44	–	98.40
A.R. Hassan et al. [59]	CEEMDAN + Linear programming boosting	98.11	96.93	97.60
Proposed method	VMD + NLTWSVM	99.28	99.66	99.57

the effectiveness of the method in this article. For the 7-class classification problem, the article uses the confusion matrix representation method and the weighted F_1 score to illustrate the effectiveness of classifying seizure types. For the 7 seizure types, the correct classification rate for this method can reach up to 0.98 and the weighted F_1 score is 0.923. This method is valuable for clinical assistant experienced neurophysiologists to identify seizure types in patients with epilepsy.

CRediT authorship contribution statement

Shang Zhang: Methodology, Software, Visualization, Writing – original draft, Writing – review & editing. **Guangda Liu:** Conceptualization, Supervision. **Ruolan Xiao:** Software. **Wenjie Cui:** Investigation. **Jing Cai:** Writing – review & editing. **Xinlei Hu:** Writing – review & editing. **Yubing Sun:** Validation. **Jiqing Qiu:** Resources. **Yuan Qi:** Resources.

Acknowledgements

The work was supported by the Science and Technology Development Plan Project of Jilin Province (20190303043SF), and the "13th Five-Year Plan" Science and Technology Project of the Education Department of Jilin Province (JJKH20200964KJ)' to the corrected content 'The work was supported by the Science and Technology Development Plan Project of Jilin Province (20190303043SF), the "13th Five-Year Plan" Science and Technology Project of the Education Department of Jilin Province (JJKH20200964KJ) and the Science and Technology Development Plan Project of Jilin Province (20200404205YY).

Conflicts of Interest

The authors declare no conflict of interest.

REFERENCES

[1] Moshe SL, Perucca E, Ryvlin P, Tomson T. Epilepsy: new advances. Lancet 2015;385(9971):884–98. https://doi.org/10.1016/s0140-6736(14)60456-6.

[2] Franco AC, Parreira S, Bentes C, Pimentel J. Management of a first unprovoked epileptic seizure in adolescence and adulthood. Epileptic Disord 2021;23(4):537–51. https://doi.org/10.1684/epd.2021.1296.

[3] WHO, Epilepsy: Fact Sheets, detail, World Health Organization, 2019. Available at: https://www.who.int/news-room/fact-sheets/detail/epilepsy.

[4] van Win OA, Barnes JG, Ferrier CF, Booth F, Prasad AN, Kasteleijn-Nolst Trenite DGA. A study of the significance of photoparoxysmal responses and spontaneous epileptiform discharges in the EEG in childhood epilepsy. Epilepsy Behav 2020;107:107046. https://doi.org/10.1016/j.yebeh.2020.107046.

[5] Sen A, Jette N, Husain M, Sander JW. Epilepsy in older people. Lancet 2020;395(10225):735–48. https://doi.org/10.1016/S0140-6736(19)33064-8.

[6] Mariam Bee MK, Vidhya K. An automated methodology for the classification of focal and nonfocal EEG signals using a hybrid classification approach. Int J Imaging Syst Technol 2020;30(1):147–53. https://doi.org/10.1002/ima.22360.

[7] Kural MA, Duez L, Sejer Hansen V, Larsson PG, Rampp S, Schulz R, et al. Criteria for defining interictal epileptiform discharges in EEG: A clinical validation study. Neurology 2020;94(20):e2139–47.

[8] Geng D, Alkhachroum A, Melo Bicchi MA, Jagid JR, Cajigas I, Chen ZS. Deep learning for robust detection of interictal epileptiform discharges. J Neural Eng 2021;18(5):056015. https://doi.org/10.1088/1741-2552/abf28e.

[9] Swami P, Gandhi TK, Panigrahi BK, Tripathi M, Anand S. A novel robust diagnostic model to detect seizures in electroencephalography. Expert Syst Appl 2016;56:116–30. https://doi.org/10.1016/j.eswa.2016.02.040.

[10] Yao X, Li X, Ye Q, Huang Y, Cheng Q, Zhang G-Q. A robust deep learning approach for automatic classification of seizures against non-seizures. Biomed Signal Process Control 2021;64:102215. https://doi.org/10.1016/j.bspc.2020.102215.

[11] Khosla A, Khandnor P, Chand T. A comparative analysis of signal processing and classification methods for different applications based on EEG signals. Biocybern Biomed Eng 2020;40(2):649–90. https://doi.org/10.1016/j.bbe.2020.02.002.

[12] Zhang Q, Ding Ji, Kong W, Liu Y, Wang Q, Jiang T. Epilepsy prediction through optimized multidimensional sample entropy and Bi-LSTM. Biomed Signal Process Control 2021;64:102293. https://doi.org/10.1016/j.bspc.2020.102293.

[13] Madhavan S, Tripathy RK, Pachori RB. Time-frequency domain deep convolutional neural network for the classification of focal and non-focal EEG signals. IEEE Sens J 2020;20(6):3078–86.

[14] Mursalin M, Zhang Y, Chen YH, Chawla NV. Automated epileptic seizure detection using improved correlation-based feature selection with random forest classifier. Neurocomputing 2017;241:204–14. https://doi.org/10.1016/j.neucom.2017.02.053.

[15] Aileni RM, Pasca S, Florescu A. EEG-brain activity monitoring and predictive analysis of signals using artificial neural networks. Sensors 2020;20(12):3346. https://doi.org/10.3390/s20123346.

[16] Dodia S, Edla DR, Bablani A, Ramesh D, Kuppili V. An efficient EEG based deceit identification test using wavelet packet transform and linear discriminant analysis. J Neurosci Methods 2019;314:31–40. https://doi.org/10.1016/j.jneumeth.2019.01.007.

[17] Samiee K, Kovacs P, Gabbouj M. Epileptic seizure classification of EEG time-series using rational discrete short-time Fourier Transform. IEEE Trans Biomed Eng 2015;62(2):541–52. https://doi.org/10.1109/tbme.2014.2360101.

[18] Kumar Y, Dewal ML, Anand RS. Epileptic seizure detection using DWT based fuzzy approximate entropy and support vector machine. Neurocomputing 2014;133:271–9. https://doi.org/10.1016/j.neucom.2013.11.009.

[19] Zhang T, Chen W. LMD based features for the automatic seizure detection of EEG signals using SVM. IEEE Trans Neural Syst Rehabil Eng 2017;25(8):1100–8.

[20] Sharma M, Pachori RB, Acharya UR. A new approach to characterize epileptic seizures using analytic time-frequency flexible wavelet transform and fractal dimension. Pattern Recognit Lett 2017;94:172–9. https://doi.org/10.1016/j.patrec.2017.03.023.

[21] Alickovic E, Kevric J, Subasi A. Performance evaluation of empirical mode decomposition, discrete wavelet transform, and wavelet packed decomposition for automated epileptic seizure detection and prediction. Biomed Signal Process Control 2018;39:94–102. https://doi.org/10.1016/j.bspc.2017.07.022.

[22] Kalbkhani H, Shayesteh MG. Stockwell transform for epileptic seizure detection from EEG signals. Biomed Signal Process Control 2017;38:108–18. https://doi.org/10.1016/j.bspc.2017.05.008.

[23] Bajaj V, Rai K, Kumar A, Sharma D. Time-frequency image based features for classification of epileptic seizures from EEG signals. Biomed Phys Eng Express 2017;3(1). https://doi.org/10.1088/2057-1976/aa5199.

[24] Seo JH, Tsuda I, Lee YJ, Ikeda A, Matsuhashi M, Matsumoto R, Kikuchi T, Kang H. Pattern recognition in epileptic EEG signals via dynamic mode decomposition. Mathematics 2020;8(4):481. https://doi.org/10.3390/math8040481.

[25] Cura OK, Akan A. Analysis of epileptic EEG signals by using dynamic mode decomposition and spectrum. Biocybern Biomed Eng 2021;41(1):28–44. https://doi.org/10.1016/j.bbe.2020.11.002.

[26] Song Y, Crowcroft J, Zhang J. Automatic epileptic seizure detection in EEGs based on optimized sample entropy and extreme learning machine. J Neurosci Methods 2012;210(2):132–46. https://doi.org/10.1016/j.jneumeth.2012.07.003.

[27] Aarabi A, He B. Seizure prediction in patients with focal hippocampal epilepsy. Clin Neurophysiol 2017;128(7):1299–307. https://doi.org/10.1016/j.clinph.2017.04.026.

[28] Bari MF, Anowarul Fattah S. Epileptic seizure detection in EEG signals using normalized IMFs in CEEMDAN domain and quadratic discriminant classifier. Biomed Signal Process Control 2020;58:101833. https://doi.org/10.1016/j.bspc.2019.101833.

[29] Beeraka SM, Kumar A, Sameer M, Ghosh S, Gupta B. Accuracy enhancement of epileptic seizure detection: A deep learning approach with hardware realization of STFT. Circuits Syst Signal Process 2022;41(1):461–84.

[30] Panda S, Das A, Mishra S, Mohanty MN. Epileptic seizure detection using deep ensemble network with empirical wavelet transform. Meas Sci Rev 2021;21(4):110–6. https://doi.org/10.2478/msr-2021-0016.

[31] Praveena HD, Subhas C, Naidu KR. Automatic epileptic seizure recognition using reliefF feature selection and long short term memory classifier. J Ambient Intell Humaniz Comput 2021;12(6):6151–67. https://doi.org/10.1007/s12652-020-02185-7.

[32] Kaur C, Bisht A, Singh P, Joshi G. EEG Signal denoising using hybrid approach of Variational Mode Decomposition and wavelets for depression. Biomed Signal Process Control 2021;65:102337. https://doi.org/10.1016/j.bspc.2020.102337.

[33] Li MY, Chen WZ, Zhang T. Application of MODWT and log-normal distribution model for automatic epilepsy identification. Biocybern Biomed Eng 2017;37(4):679–89. https://doi.org/10.1016/j.bbe.2017.08.003.
[34] Sameer M, Gupta B. Detection of epileptical seizures based on alpha band statistical features. Wirel Pers Commun 2020;115 (2):909–25. https://doi.org/10.1007/s11277-020-07542-5.
[35] Siuly S, Alcin OF, Bajaj V, Sengur A, Zhang Y. Exploring Hermite transformation in brain signal analysis for the detection of epileptic seizure. IET Sci Meas Technol 2019;13 (1):35–41. https://doi.org/10.1049/iet-smt.2018.5358.
[36] Zhang T, Chen W-Z, Li M-Y. Automatic seizure detection of electroencephalogram signals based on frequency slice wavelet transform and support vector machine. Acta Phys Sin 2016;65(3):038703. https://doi.org/10.7498/aps.65.038703.
[37] Song J-L, Zhang R. Application of extreme learning machine to epileptic seizure detection based on lagged Poincare plots. Multidimens Syst Signal Process 2017;28(3):945–59. https://doi.org/10.1007/s11045-016-0419-y.
[38] Jia J, Goparaju B, Song J, Zhang R, Westover MB. Automated identification of epileptic seizures in EEG signals based on phase space representation and statistical features in the CEEMD domain. Biomed Signal Process Control 2017;38:148–57. https://doi.org/10.1016/j.bspc.2017.05.015.
[39] Li Y, Wang X-D, Luo M-L, Li Ke, Yang X-F, Guo Qi. Epileptic seizure classification of EEGs using time-frequency analysis based multiscale radial basis functions. IEEE J Biomed Health Inform 2018;22(2):386–97.
[40] Huang NE, Shen Z, Long SR, Wu MC, Shih HH, Zheng Q, et al. The empirical mode decomposition and the Hilbert spectrum for nonlinear and non-stationary time series analysis. Proc R Soc Lond A 1998;454(1971):903–95.
[41] Muñoz-Gutiérrez PA, Giraldo E, Bueno-López M, Molinas M. Localization of active brain sources from EEG signals using empirical mode decomposition: A comparative study. Front Integr Neurosci 2018;12:55. https://doi.org/10.3389/fnint.2018.00055.
[42] Wu Z, Huang NE. Ensemble empirical mode decomposition: A noise-assisted data analysis method. Adv Adapt Data Anal 2009;01(01):1–41. https://doi.org/10.1142/s1793536909000047.
[43] Hassan AR, Subasi A, Zhang Y. Epilepsy seizure detection using complete ensemble empirical mode decomposition with adaptive noise. Knowl-Based Syst 2020;191:105333. https://doi.org/10.1016/j.knosys.2019.105333.
[44] Dragomiretskiy K, Zosso D. Variational mode decomposition. IEEE Trans Signal Process 2014;62(3):531–44. https://doi.org/10.1109/tsp.2013.2288675.
[45] Rout SK, Sahani M, Dash PK, Biswal PK. Multifuse multilayer multikernel RVFLN plus of process modes decomposition and approximate entropy data from iEEG/sEEG signals for epileptic seizure recognition. Comput Biol Med 2021;132. https://doi.org/10.1016/j.compbiomed.2021.104299 104299.
[46] Andrzejak RG, Lehnertz K, Mormann F, Rieke C, David P, Elger CE. Indications of nonlinear deterministic and finite-dimensional structures in time series of brain electrical activity: Dependence on recording region and brain state. Phys Rev E 2001;64(6). https://doi.org/10.1103/PhysRevE.64.061907.
[47] Shah V, von Weltin E, Lopez S, McHugh JR, Veloso L, Golmohammadi M, et al. The Temple University Hospital Seizure Detection Corpus. Front Neuroinf 2018;12(83). https://doi.org/10.3389/fninf.2018.00083.
[48] Yadav VP, Sharma KK. Variational mode decomposition-based seizure classification using Bayesian regularized shallow neural network. Biocybern Biomed Eng 2021;41 (2):402–18. https://doi.org/10.1016/j.bbe.2021.02.003.
[49] Carvalho VR, Moraes MFD, Braga AP, Mendes EMAM. Evaluating five different adaptive decomposition methods for EEG signal seizure detection and classification. Biomed Signal Process Control 2020;62:102073. https://doi.org/10.1016/j.bspc.2020.102073.
[50] Rezvani S, Wang X, Pourpanah F. Intuitionistic fuzzy twin support vector machines. IEEE Trans Fuzzy Syst 2019;27 (11):2140–51.
[51] Guan S, Zhao K, Wang F. Multiclass motor imagery recognition of single joint in upper limb based on NSGA- II OVO TWSVM. Comput Intell Neurosci 2018;2018:1–11. https://doi.org/10.1155/2018/6265108.
[52] Sukriti, Chakraborty M, Mitra D. Mitra, Epilepsy seizure detection using kurtosis based VMD's parameters selection and bandwidth features. Biomed Signal Process Control 2021;64:102255. https://doi.org/10.1016/j.bspc.2020.102255.
[53] Zeng W, Yuan J, Yuan C, Wang Q, Liu F, Wang Y. Classification of myocardial infarction based on hybrid feature extraction and artificial intelligence tools by adopting tunable-Q wavelet transform (TQWT), variational mode decomposition (VMD) and neural networks. Artif Intell Med 2020;106:101848. https://doi.org/10.1016/j.artmed.2020.101848.
[54] Zhou DM, Li XM. Epilepsy EEG signal classification algorithm based on improved RBF. Front Neurosci 2020;14:7. https://doi.org/10.3389/fnins.2020.00606.
[55] Raghu S, Sriraam N. Optimal configuration of multilayer perceptron neural network classifier for recognition of intracranial epileptic seizures. Expert Syst Appl 2017;89:205–21. https://doi.org/10.1016/j.eswa.2017.07.029.
[56] Gupta A, Singh P, Karlekar M. A novel signal modeling approach for classification of seizure and seizure-free EEG signals. IEEE Trans Neural Syst Rehabil Eng 2018;26(5):925–35.
[57] Raghu S, Sriraam N, Hegde AS, Kubben PL. A novel approach for classification of epileptic seizures using matrix determinant. Expert Syst Appl 2019;127:323–41. https://doi.org/10.1016/j.eswa.2019.03.021.
[58] Mathur P, Chakka VK, Shah SB. Ramanujan periodic subspace based epileptic EEG signals classification. IEEE Sens Lett 2021;5(7):1–4.
[59] Hassan AR, Subasi A. Automatic identification of epileptic seizures from EEG signals using linear programming boosting. Comput Meth Programs Biomed 2016;136:65–77. https://doi.org/10.1016/j.cmpb.2016.08.013.
[60] Sharma M, Bhurane AA, Acharya UR. MMSFL-OWFB: A novel class of orthogonal wavelet filters for epileptic seizure detection. Knowl-Based Syst 2018;160:265–77. https://doi.org/10.1016/j.knosys.2018.07.019.
[61] Jaiswal AK, Banka H. Local pattern transformation based feature extraction techniques for classification of epileptic EEG signals. Biomed Signal Process Control 2017;34:81–92. https://doi.org/10.1016/j.bspc.2017.01.005.
[62] Patidar S, Panigrahi T. Detection of epileptic seizure using Kraskov entropy applied on tunable -Q wavelet transform of EEG signals. Biomed Signal Process Control 2017;34:74–80. https://doi.org/10.1016/j.bspc.2017.01.001.
[63] Mandhouj B, Cherni MA, Sayadi M. An automated classification of EEG signals based on spectrogram and CNN for epilepsy diagnosis. Analog Integr Circuits Process 2021;108(1):101–10. https://doi.org/10.1007/s10470-021-01805-2.
[64] Zhao W, Wang W. SeizureNet: a model for robust detection of epileptic seizures based on convolutional neural network. Cogn Comput Syst 2020;2(3):119–24. https://doi.org/10.1049/ccs.2020.0011.
[65] Murugavel ASM, Ramakrishnan S. Hierarchical multi-class SVM with ELM kernel for epileptic EEG signal classification. Med Biol Eng Comput 2016;54(1):149–61. https://doi.org/10.1007/s11517-015-1351-2.
[66] Jiang Y, Chen W, Li M, Zhang T, You Y. Synchroextracting chirplet transform-based epileptic seizures detection using

EEG. Biomed Signal Process Control 2021;68:102699. https://doi.org/10.1016/j.bspc.2021.102699.

[67] Ahmedt-Aristizabal D, Fernando T, Denman S, Petersson L, Aburn MJ, Fookes C. Neural memory networks for seizure type classification. In: Annual International Conference of the IEEE Engineering in Medicine and Biology Society. IEEE Engineering in Medicine and Biology Society. Annual International Conference. p. 569–75. https://doi.org/10.1109/EMBC44109.2020.9175641.

[68] McCallan N, Davidson S, Ng KY, Biglarbeigi P, Finlay D, Lan BL, et al. Seizure classification of EEG based on wavelet signal denoising using a novel channel selection algorithm (In Press). 13th Asia Pacific Signal and Information Processing Association Annual Summit and Conference (APSIPA ASC), 2021.

[69] Asif U, Roy S, Tang J, Harrer S, SeizureNet: Multi-spectral deep feature learning for seizure type classification, arXiv e-prints (2019) arXiv:1903.03232.

[70] Fukumori K, Yoshida N, Tanaka T, Epileptic spike detection by recurrent neural networks with self-attention mechanism, bioRxiv (2021.06.17) 448793, https://dx.doi.org/10.1101/2021.06.17.448793.

[71] Lourenco C, Tjepkema-Cloostermans MC, Teixeira LF, van Putten M. Deep learning for interictal epileptiform discharge detection from scalp EEG recordings. In: 15th Mediterranean Conference on Medical and Biological Engineering and Computing (MEDICON). Coimbra, Portugal: Springer International Publishing Ag, UNESCO World Heritage Univ; 2019. p. 1984–97.

[72] Baud MO, Schindler K, Rao VR. Under-sampling in epilepsy: Limitations of conventional EEG. Clin Neurophys Pract 2021;6:41–9. https://doi.org/10.1016/j.cnp.2020.12.002.

[73] Proix T, Truccolo W, Leguia MG, Tcheng TK, King-Stephens D, Rao VR, et al. Forecasting seizure risk in adults with focal epilepsy: a development and validation study. Lancet Neurol 2021;20(2):127–35.

[74] Turco F, Bonanni E, Milano C, Pizzanelli C, Steinwurzel C, Morganti R, et al. Prolonged epileptic discharges predict seizure recurrence in JME: Insights from prolonged ambulatory EEG. Epilepsia 2021;62(5):1184–92. https://doi.org/10.1111/epi.16875.